A&A 456, 775–781 (2006)
DOI: 10.1051/0004-6361:20054347

Astronomy & Astrophysics

Basaltic asteroids in the Near-Earth Objects population: a mineralogical analysis⋆

R. Duffard[1,⋆⋆], J. de León[2], J. Licandro[3,2], D. Lazzaro[1], and M. Serra-Ricart[3]

[1] Observatório Nacional - MCT, Rua Gal. José Cristino 77, Rio de Janeiro, 20921-400 RJ, Brazil
e-mail: duffard@mps.mpg.de
[2] Instituto de Astrofísica de Canarias, c/ vía Láctea s/n, 38200 La Laguna, Tenerife, Spain
[3] Isaac Newton Group, PO Box 321, 38700 Santa Cruz de La Palma, La Palma, Spain

Received 13 October 2005 / Accepted 20 April 2006

ABSTRACT

Aims. We present reflectance spectra of three V-type Near-Earth Objects obtained at the 3.6 m Telescopio Nazionale Galileo and at the 2.5 m Nordic Optical Telescope covering the near-infrared and visible range, respectively. The range from 0.5 to 2.5 μm, encompassing the 1 and 2 μm pyroxene features, allows a mineralogical characterization of these asteroids.
Methods. A preliminary analysis using the classical methods has been applied to establish some constraints on the surface mineralogy of these objects. Then, the Modified Gaussian Method was applied to gain further insight on the possible mineral components present in the surface of the objects.
Results. The comparison between these basaltic asteroids in near Earth orbits and the achondrite basaltic meteorites shows a quite clear mineralogical link, corroborating the long-standing hypothesis of the Near-Earth Objects population as the immediate source of these meteorites.

Key words. minor planets, asteroids

1. Introduction

One of the most important issues in the study of Near-Earth objects (NEOs) is to understand their origin and their possible connection with meteorites. In this sense, we note that the planet-crossing asteroids, Aten, Apollo and Amor, are believed to be primary reservoirs for meteorites. The comparison of the spectral characteristics of these two populations, NEOs and meteorites, with those of main belt asteroids, can provide clues on the possible mineralogical relationship between these populations. A mineralogical link can then help constrain the possible transport routes that might deliver meteorites to the Earth. Specifically, since the basaltic NEOs have a V-type taxonomic classification, they are good spectral matches to the Howardite-Eucrite-Diogenites (HED) meteorites, to asteroid (4) Vesta, and to other V-type asteroids in the main belt.

Recently, several works have been devoted to the study of the mineralogy of V-type asteroids, probing the hypothesis of an unique origin. Kelley et al. (2003) analysed the pyroxene chemistry of asteroid (1929) Kollaa, a member of the Vesta dynamical family. They concluded that the mineralogy of this asteroid is very similar to the average of Vesta's crust, as derived frompreviously studies (Gaffey et al. 1993; Gaffey 1997), and the pyroxene present falls well within the range of basaltic achondrite meteorites. On the other hand, Hardersen et al. (2004) show that the outer main belt basaltic asteroid (1459) Magnya presents a quite distinct pyroxene, with less iron content. Their primary conclusion is that (1459) Magnya is probably not related to (4) Vesta. The study of 19 V-type asteroids in the neighbourhood of Vesta (Duffard et al. 2004) also confirms the existence of different kinds of basalts, but with no clear correlation between mineralogies and membership to the Vesta's dynamical family. Finally, Duffard et al. (2005) analysed a number of HED meteorites taken from the Reflectance Experiment Laboratory (RELAB) database[1], redefining the regions where the different meteorite classes plot in spectral parameter space.

Cruikshank et al. (1991) suggested that the V-type NEOs (3551) Verenia, (3908) Nyx, and (4055) Magellan were ejected fragments from the disruption of a Vesta clone, but not of Vesta itself. On the other hand, Migliorini et al. (1997) presented a kind of a paradox consisting of the fact that the seven V-type NEOs known at that time appeared to be too young, from a dynamical point of view, to have originated in the event that produced the Vesta family. At the same time, they were too big to be plausible second-generation fragments. Currently, according to the list of Physical Parameters of NEOs published in Binzel et al. (2002), we know 16 NEOs with a V-type spectra.

In this work we analyse the mineralogy of three V-type NEOs, two of them previously unclassified with the aim of understanding their possible link to Vesta and to the HED meteorites. This analysis will be performed using two different

⋆ Based on observations made with the Nordic Optical Telescope (NOT), operated on the island of La Palma jointly by Denmark, Finland, Iceland, Norway, and Sweden, and on observations made with the Italian Telescopio Nazionale Galileo (TNG) operated on the island of La Palma by the Centro Galileo Galilei of the INAF (Istituto Nazionale di Astrofisica), both telescopes are located at the Spanish Observatorio de El Roque de los Muchachos of the Instituto de Astrofisica de Canarias.

⋆⋆ *Present address*: Max Planck Institute for Solar System Research, Max-Planck-Str. 2, Katlenburg-Lindau 37191, Germany.

[1] www.planetary.brown.edu/relab

Table 1. Orbital parameters of the asteroids.

Asteroid name	Group	H	q [AU]	Q [AU]	a (AU)	e	incl.
(6611) 1993 VW	Apollo	16.5	0.873	2.516	1.695	0.485	8.7
(88188) 2000 XH44	Amor	16.0	1.218	2.795	2.007	0.393	11.4
2003 YG118	Apollo	17.1	0.812	3.754	2.283	0.644	8.1

Table 2. Observational parameters of the asteroids.

NIR observations Asteroid	Date	UT-start	Airmass	r (AU)	Δ (AU)	Phase angle	# AB	Total exp. time [s]
(6611) 1993 VW	24/06/03	01:54	1.27	1.936	0.986	15.0	36	3240
2003 YG118	15/01/04	22:17	1.15	1.687	0.723	10.1	12	1080
(88188) 2000 XH44	16/01/04	05:42	1.10	2.078	2.722	18.0	4	360
Visible observations Asteroid	Date	UT-start	Airmass	r (AU)	Δ (AU)	Phase angle	#	Total exp. time [s]
2003 YG118	16/01/04	1:21	1.02	1.686	0.722	10.1	2	2000
(88188) 2000 XH44	16/01/04	5:14	1.05	2.078	2.722	18.0	1	900

The column # AB is the number of individual expositions of 90 s taken in position A or B.

methods to better assess the surface mineralogy of the observed asteroids.

2. Observations and reduction

The 3.6 m Telescopio Nazionale Galileo (TNG) and the 2.5 m Nordic Optical Telescope (NOT) at El Roque de los Muchachos Observatory were used to observe three NEOs as part of an extensive campaign to obtain visible and near-infrared reflectance spectra of a large number of NEOs (de León et al. 2003). The orbital parameters of the observed asteroids are given in Table 1, while the observational data is given in Table 2.

Low resolution spectra in the near-infrared region of asteroids (88188) 2000 XH44, 2003 YG118, and (6611) 1993 VW were obtained with the TNG using NICS, the near-infrared camera and spectrometer. Among the many imaging and spectroscopic observing modes, NICS offers a unique, high throughput, low resolution spectroscopic mode with an Amici prism disperser (Baffa et al. 2001), which yields a complete 0.8–2.4 μm spectrum. A 1.5″ width slit, oriented in the paralactic angle, corresponding to a quasi-constant spectral resolving power R ranging from $R \sim 25$ to $R \sim 45$ along the spectrum, was used[2]. The identification of the asteroids was done by taking series of images through the J_s filter and by comparing them. The asteroid was identified as a moving object at the predicted position and with the predicted proper motion. The slit was oriented in the parallactic angle, and the tracking was at the asteroid proper motion.

The observing and reduction procedures were as described in Licandro et al. (2002). The acquisition consisted of a series of images exposed 90 s in one position of the slit (position A) and then the telescope was offset by 10″ in the direction of the slit (position B). This process was repeated and a number of $ABBA$ cycles were acquired. The total exposure time is given in Table 2. The reduction of the spectra was done by subtracting consecutive A and B images. Each A-B frame had some residual of sky emission, related to sky transparency fluctuations and/or intrinsic variation of the air-glow atmospheric emission, which was eliminated by extracting the "short-slit" spectrum around each A B spectrum, then aligning and combining them into the final short-slit spectrum from which the 1D spectra were extracted. No contribution from residual sky emission was found within the noise of the spectra. Wavelength calibration was performed by using the look-up table included in NICS web page, which is based on the theoretical dispersion predicted by ray-tracing. Sub-pixel offsets are applied to fit the observed spectra of an Argon lamp and the deep telluric absorption features. An uncertainty <0.003 microns is expected.

To correct for telluric absorption and to obtain the relative reflectance, the G2-type stars Landolt 110–361, Landolt 112–1333, and Landolt 115–271 (Landolt 1992) were observed on June 24, 2003, while Landolt 107–998, Landolt 102–1081, and Landolt 93–101 were observed on Jan. 15, 2004 at different airmasses. These stars were observed in previous nights and compared to the spectrum also obtained of the solar analogue star P330E (Colina & Bohlin 1997) and all presented similar spectra in the infrared region within the resolving power of our system, so we used them as solar analogues. The spectrum of each asteroid was divided by the spectra of all solar analogue stars and normalised to unity at 1.6 μm. Further sub-pixel offsetting was applied to the asteroid spectrum when dividing it against the solar analogs to deal with the uncertainties in the wavelength calibrations that can produce false features like in Fig. 2 of Gaffey et al. (2002). Differences in atmospheric extinction during the asteroid and standard star observations produce false absorption or "emission" bands in the computed reflectance spectrum of the asteroids, around the deep atmospheric telluric band spectral regions. The large spectral coverage of the Amici prism allow us to easily detect them. We correct this effect by multiplying the reflectance spectrum by SA^f/SA, where SA is the spectrum of the solar analogue star and f is a number usually close to 1. Different f numbers are used until the "false" features disappear. We finally computed the mean of the normalised spectra to obtain a final relative reflectance spectrum for each asteroid.

By dividing the spectra of Landolt 110−361 and Landolt 112−1333 by the spectrum of Landolt 115−271 obtained on June 24, 2003, and by dividing the spectra of Landolt 107–998 and Landolt 102–1081, by the spectrum of

[2] www.tng.iac.es/instruments/nics/images/grisms_all.gif

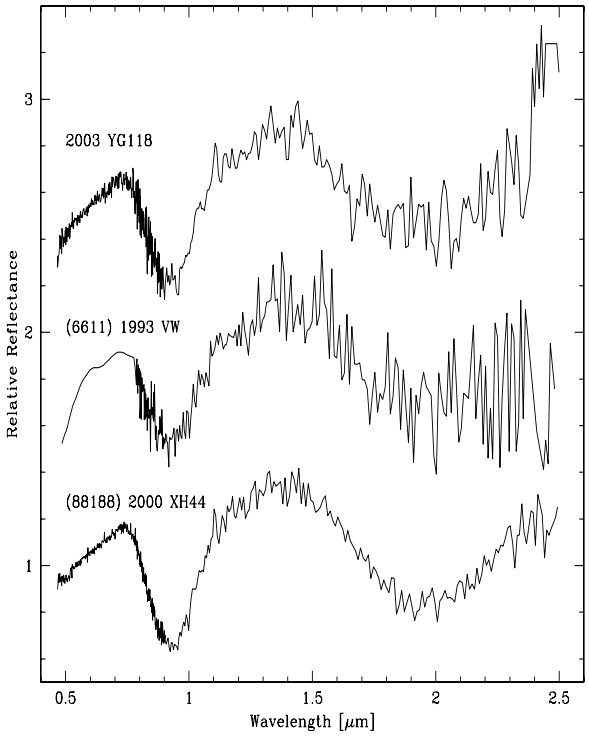

Fig. 1. Visible and near infrared spectrum of the observed asteroids. All spectra have been normalised to unity at 0.55 μm and offset vertically for clarity.

Landolt 93–101 obtained on Jan. 15, 2004, and then normalising to unity around 1.6 μm, we obtained featureless spectra with slope 0 ± 0.37%/1000 Å. From this we conclude that atmospheric conditions were very stable during both nights and the uncertainty in the slope of the reflectance spectra of the asteroids is smaller than 0.4%/1000 Å.

Visible spectra of 2003 YH118 and (88188) 2000 XH44 were obtained with the NOT using the Andalucia Faint Object Spectrograph and Camera (ALFOSC). We used a grism disperser with a wavelength range of 0.32–0.91 μm ($\lambda_{\rm cent}$ = 0.58 μm) and a second order blocking filter (cut-off wavelength at 0.47 μm). A 1.3″ slit was used. As in the infrared observations, the slit was oriented in the parallactic angle and the tracking was at the object proper motion. The spectral data reduction was done using the Image Reduction and Analysis Facility (IRAF) package, following standard procedures. Images were over-scan and bias corrected, and flat-field corrected using lamp flats. The two-dimensional spectra were extracted, sky background subtracted, and collapsed to one dimension. Wavelength calibration was performed using a helium-neon lamp and two solar analog stars (Landolt 115−271 and Landolt 110−361) were observed to correct for telluric absorption and to obtain the reflectance spectrum of the asteroid, as was done in the near-infrared. Finally, the visible spectra were normalised to unity at 0.55 μm.

To analyse the complete VNIR spectrum, we first overlap the visible and near-infrared spectra using the common interval between 0.78 and 0.90 μm by performing a least-square minimum procedure. The near-infrared spectra were re-normalised to join the visible spectra and are shown in Fig. 1 normalised to unity at 0.55 μm and offset vertically for clarity. In the case of (6611) 1993 VW, the visible spectrum was taken from Di Martino et al. (1995).

3. Analysis of the data and discussion

The silicate mineralogical composition of the surface of an asteroid can be obtained through the analysis of its spectrum in the visible and near-infrared (VNIR) region. As described in the previous section, our observations of the three NEOs consisted of a visible (for two of them) and near infrared spectrum with useful ranges from 0.5 to 0.9 μm and from 0.78 to 2.5 μm, respectively.

The VNIR reflectance spectra of the three objects (Fig. 1) exhibit broad absorption features near 1- and 2-μm (Band I and Band II, respectively) that are typical of rocks dominated by mafic silicates. The combination of pyroxenes has been described as having spectral properties that are intermediate between those of low-calcium (orthopyroxene or LCP) and high-calcium (clinopyroxene or HCP) (Adams 1974; Cloutis & Gaffey 1991).

A calibration between abundance in olivine-orthopyroxene (Ol-LCP) mixtures and the ratios of areas for the 1- and 2-μm absorption bands was developed by Cloutis et al. (1986). On the other hand, the relationship between diagnostic spectral parameters (band centre positions and band areas) for reflectance spectra of a number of mafic minerals, particularly pyroxene and olivine, was outlined by Adams (1974, 1975) and revisited by King & Ridley (1987), Cloutis & Gaffey (1991), and Gaffey et al. (2002). Therefore, we started the mineralogical analysis of our spectra by using this method as outlined in Gaffey et al. (2002), identified as G02 in what follows.

To further constrain the pyroxene signature present in the spectra of the observed objects, we then used the Modified Gaussian Model (MGM), developed by Sunshine et al. (1990), identified as S90 in what follows. This method performs a spectral deconvolution by means of representing absorption bands as discrete mathematical distributions and resolves composite absorption features into individual absorption bands superimposed onto a background continuum.

3.1. First mineralogical analysis

Among the most important parameters that can be extracted from the kind of spectra that our objects have are the positions of the centres of the absorption bands near 1 and 2 μm, the band areas, and the band areas ratio (BAR). A detailed discussion of the definition and mineralogical information associated with each of these parameters can be found in G02.

Using the complete VNIR reflectance spectra, we determined the reflectance values and positions of the two maxima, near 0.7 and 1.4 μm, and computed a linear continuum in this region. Similar procedure was used in the interval between 1.4 and around 2.4 μm. The obtained continua were then extracted from the spectra by dividing each linear continuum in the corresponding region for each object. We note that, although the initial method by Cloutis et al. (1986) required setting a limiting point at 2.4 μm, more recent works have used the longest "good" point of the spectra. The 2.4 μm option somewhat increases the uncertainty in the mineral abundance determination, but on the other hand, has the advantage of allowing a secure comparison between values obtained by diverse authors. Since most of the published values for basaltic asteroids were obtained using the longest "good" point of the spectra, we decided to compute the Band II area using this method. However, we also computed values using the "limiting" point of the original method. This has been done to show how the BAR is affected by the adopted limiting point.

Table 3. Spectral parameters for the observed NEOs compared with the asteroids (4) Vesta, (1459) Magnya, (4188) Kitezh, and the eucrite meteorite Bouvante. The BAR values in parenthesis are given using the 2.4 μm limiting point, as explained in the text.

Using Cloutis et al. (1986) and Gaffey et al. (2002)	(88188) 2000 XH44	2003 YG118	(6611) 1993 VW	(4) Vesta [a]	(4) Vesta [b]	(1459) Magnya [c]
Band I centre [μm]	0.932 ± 0.008	0.926 ± 0.010	0.931 ± 0.010	0.936 ± 0.001	0.924 ± 0.002	0.925 ± 0.003
Band II centre [μm]	1.952 ± 0.025	1.932 ± 0.04	1.945 ± 0.04	1.969 ± 0.005	1.960 ± 0.03	1.932 ± 0.010
BAR	2.00 (1.88)	2.44 (1.66)	1.49 (1.23)	2.74	2.05–2.68	3.4–4.3
[Wo](mol%)	9 ± 4	7 ± 4	9 ± 4	8 ± 4	6 ± 4	8 ± 4
[Fs](mol%)	39 ± 5	34 ± 5	37 ± 5	46 ± 5	34 - 51 ± 5	36 ± 5
Using MGM				(4) Vesta [b]	(4188) Kitezh [d]	Bouvante [d]
Band I centre [μm]	0.923 ± 0.005	0.918 ± 0.005	0.919 ± 0.008			
Band II centre [μm]	1.945 ± 0.005	1.909 ± 0.005	1.90 ± 0.008			
CBSR	2.63–3.57	1.82–3.66	2.32–2.46	3.0–2.73	2.5–3.6	2.3–3.3
HCP/(HCP+LCP)	0.27–0.36	0.27–0.48	0.38–0.40	0.15–0.38	0.27–0.39	0.29–0.42

[a] Gaffey (1997); [b] Vernazza et al. (2005); [c] Hardersen et al. (2004); [d] Sunshine et al. (2004).

The obtained spectra after the removal of the continuum were used to compute the band centres and band areas. The centre determination was done by fitting a second order polynomial in the region of the minimum. The error in the position of the centres has been obtained by propagating the errors of the individual points with those of the parabola fitting procedure. Finally, following G02, the band area is defined as the area enclosed by the spectral curve and a straight line tangent to the respective maxima. Band area I is between the maxima at 0.7 and 1.4 μm, and Band area II is between 1.4 and about 2.4 μm. The ratio between Band area II and Band area I is defined as the BAR parameter.

All the above parameters have been computed for our spectra of (88188) 2000 XH44, 2003 YG118, and (6611) 1993 VW and are presented in the upper part of Table 3 along with the available values for (4) Vesta, taken from Gaffey (1997) and Vernazza et al. (2005), and the average value for (1459) Magnya, from Hardersen et al. (2004). The BAR value in parenthesis was obtained using the 2.4 μm limiting point, as discussed above. In this table, the Ca^{2+}, [Wo], and Fe^{2+}, [Fs], content of pyroxene were computed using the equations outlined in G02. As noted in that paper, there is a systematic uncertainty of approximately ±5% in the compositional determinations due to the limitations in the calibrations between band position and mineral chemistry. It is also very important to note that these calibrations assume the presence of a single pyroxene and will fail when more than one kind of pyroxene is present.

As can be seen in Table 3, the mean Band I centre value for the three asteroids is around 0.93 μm, which is compatible, within the errors, to that of (4) Vesta and (1459) Magnya. The Band II centre value for the three asteroids shows a somewhat greater dispersion, varying between 1.93 and 1.95 μm, but again, in the same range as the other basaltic asteroids. The same can be said about the BAR value, although, as mentioned above, this value is strongly affected by the adopted limiting point. This occurs because a shift in the position of the adopted limiting point will increase or decrease the Band area II and, consequently, the BAR value. In the case of [Wo] and [Fs] contents, all the values given are very similar when the associated errors are considered.

Another point to analyse is the correlation between the mineralogy of the observed asteroids and that of the HED meteorites. This has been done in Fig. 2, where the values of the Band I centre and Band II centre of the observed asteroids, along with a sketch of the region encompassed by the Eucrite and Diogenite basaltic achondrite assemblages as given by Duffard et al. (2005), are plotted. We recall that the Howardites are

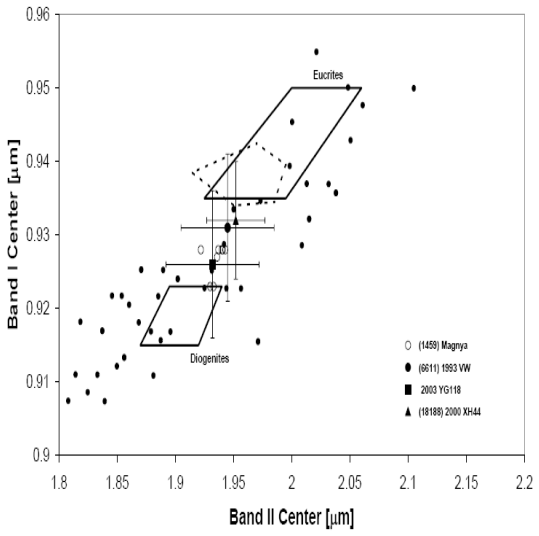

Fig. 2. Band II centre vs. Band I centre for the observed V-type NEOs. The regions corresponding to the Eucrites (Euc) and the Diogenites (Dio) meteorites are indicated in the plot (Duffard et al. 2005). Howardites are composed of Eucrite and Diogenite material and, therefore, their assemblages occupy the region in-between those of the Eucrite and the Diogenite. The values of (4) Vesta (dashed region) and for (1459) Magnya are from Gaffey (1997) and from Hardersen et al. (2004), respectively. The Magnya data are temperature corrected relative to (4) Vesta. Small filled circles are terrestrial pyroxenes taken from Cloutis & Gaffey (1991).

breccias composed of Eucrite and Diogenite and, therefore, their assemblages occupy the region in-between those of the Eucrite and the Diogenite. The data from the NEOs plots in the howardite region. Values of terrestrial pyroxenes (Cloutis & Gaffey 1991) and rotational spectra for (4) Vesta (Gaffey 1997) and (1459) Magnya (Hardersen et al. 2004) were included for comparison. The possible influence of the difference in temperature between the asteroid surfaces and their analog materials must not be ignored, the spectra of the latter being commonly recorded at ambient temperature. According to the crystal field theory it is expected that a decrease in temperature results in narrowing the absorption bands (Burns 1970) and in shifting the band centres to shorter wavelengths. Temperature variations between objects in the main belt are not important (note that the Magnya's points given in Hardersen's work have been temperature-corrected with respect to Vesta), but comparisons

with the calibrations obtained in the laboratory should consider this point. Therefore, the points for all the asteroids in Fig. 2 might be slightly shifted up and to the right of the given positions, according to Moroz et al. (2000); in this case, the Band I and Band II centres for orthopyroxene move to longer wavelengths by nearly 0.003 and 0.02 μm, respectively, values that are smaller than our error bars.

The parameter BAR can also give information about the abundance of olivine. For pure olivine this parameter is essentially zero for all the phases; however, it increases for olivine-orthopyroxene mixtures due to the presence of the second absorption band associated with pyroxene. The BAR value for (6611) 1993 VW is interestingly low, which would indicate an elevated abundance of olivine, not observed in basaltic achondrite meteorites. A significant amount of olivine would be highlighted in the band-band data (Fig. 2) where the point should be off the pyroxene trend. On the other hand, it must be noted that a mixture of low- and high-calcium pyroxene can give a BAR value similar to a mixture of olivine and low-calcium pyroxene (Sunshine et al. 2002). Comparing the values of Band I centre and BAR for the three NEOs with the LCP/HCP mixing lines given in Duffard et al. (2005), we note that (88188) 2000 XH44 fits a relation of 75/25% and a grain size between 70 and 145 μm. On the other hand, 2003 YG118 and (6611) 1993 VW fit with a LCP/HCP relation of 85/15% and 60/40%, respectively, both with a grain size smaller than 25 μm.

The obtained values seem to indicate that the surface of the three NEOs can indeed be composed of a mixture of high and low calcium pyroxene. To further constrain this result, we decided to perform a new analysis using the Modified Gaussian Model (MGM) developed by S90 and discussed below.

3.2. Second mineralogical analysis

Using the MGM method, the spectra of both LCP and HCP can be modelled with a total of seven primary absorption bands (Sunshine & Pieters 1993, SP93 in what follows). The strongest primary absorptions bands of the LCP occur at 0.91 and at 1.83 μm, while those of the HCP occur at 1.01 and at 2.27 μm, plus an additional minor absorption near 1.2 μm. The MGM method needs initial values for the strengths, widths, and centres of the different individual absorption bands for different elements, i.e., orthopyroxene, clinopyroxene, and/or olivine.

The Band I and Band II centres of the three observed NEOs are close to 0.91 and 1.83 μm, respectively, which are compatible with low-calcium pyroxene. Therefore, we initially fitted the spectra using the individual band parameters of an LCP ($Wo_{0.78}$ $En_{87.03}$ $Fs_{12.19}$), as given by SP93. The resulting best fit returned bands widths not compatible with the laboratory calibrations (S90 and SP93) and a residue with structures. According to the MGM method, these facts indicate that the fit is not acceptable, and this can be due to the unaccounted presence of an amount of high-calcium pyroxene.

One major conclusion obtained by S90 and SP93, using mixtures with different proportions of LCP and HCP, is that while the relative primary band strengths change systematically with the proportion of HCP, the primary band centres and widths remain essentially constant and all the parameters are independent of the grain size. The combination of the primary bands of the LCP (0.91 μm) and those of the HCP (1.01 and 1.2 μm) form the complex Band I. Similar effect is observed for Band II with the primary band at 1.83 (LCP) and at 2.27 μm (HCP). When the amount of HCP relative to LCP increases, the observed net effect

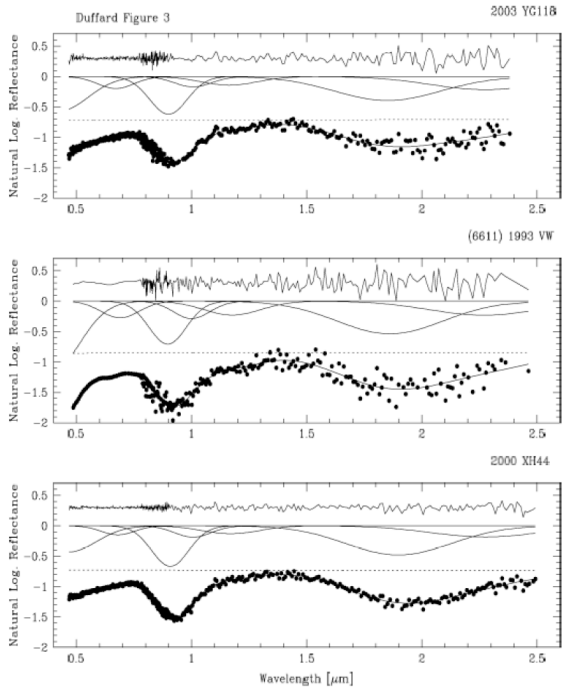

Fig. 3. MGM fit for the three observed asteroids, showing the spectra, the fit (solid line), the continuum (dashed line), the fitted individual bands, and the residual (all spectra have been normalised to unity at 0.55 μm and offset vertically for clarity).

is a shift of the Band I and Band II centres to longer wavelengths, as already shown by Adams (1974) and Cloutis & Gaffey (1991).

Since the Band I and Band II centres of the observed objects are closer to 0.91 and 1.83 μm, respectively, this indicates the presence of a higher quantity of LCP relative to HCP (Adams 1974; Cloutis & Gaffey 1991). We used the individual band parameters for the LCP ($Wo_{0.78}$ $En_{87.03}$ $Fs_{12.19}$) and HCP ($Wo_{45.59}$ $En_{45.89}$ $Fs_{8.52}$) given by SP93 as starting parameters in the MGM iteration. Considering all the necessary laboratory calibrations and initial values corresponding to a mixture of 75% LCP and 25% HCP (SP93), we begin the procedure to fit the spectra of our asteroids.

Note, however, that while band centres and band widths remain fixed, the strengths of the primary absorption bands in the LCP-HCP mass fraction mixtures appear to vary systematically with modal abundances. A value that can be used to quantify the relative strength of the primary pyroxene absorption bands is the "component band strength ratio" (CBSR). This is the band strength of the LCP component divided by the band strength of the HCP component, as defined by SP93. A CBSR value in the 1 μm and 2 μm region can be obtained and these values must be similar. The CBSR, therefore, gives us the proportion of HCP relative to LCP present in the mixture. We use this constraint to know when we must stop the iteration and verify if our fit is acceptable. Finally, using the calibrations by SP93, who plotted the systematic variation in the relative strength of pyroxene absorptions as a function of HCP/(HCP+LCP) ratios, we determine the percentage of HCP relative to LCP. The final fit for the three objects is shown in Fig. 3, while the computed parameters are presented in the lower part of Table 3 and the individual band parameters are presented in Table 4. The CBSR values computed are for the 1 and 2 μm regions, respectively.

The MGM analysis for our asteroids results in a HCP/(HCP+LCP) ratio of 0.31–0.39, which could be

Table 4. Final band parameters from MGM applied to the three asteroids using LCP and HCP.

(88188) 2000 XH44	Centre (μm)	*FWHM* (μm)	Strength (natural log)	Continuum and error in fit
Band 1	0.456	0.281	–0.43	
Band 2	0.666	0.158	–0.15	Offset
Band 3	0.903	0.197	–0.59	0.47
Band 4	0.985	0.188	–0.22	Slope
Band 5	1.165	0.289	–0.12	–1.15E-06
Band 6	1.903	0.534	–0.47	Error
Band 7	2.262	0.563	–0.17	3%
2003 YG118	Centre (μm)	*FWHM* (μm)	Strength (natural log)	Continuum and error in fit
Band 1	0.428	0.281	–0.56	
Band 2	0.658	0.159	–0.19	Offset
Band 3	0.900	0.199	–0.52	0.48
Band 4	0.980	0.186	–0.26	Slope
Band 5	1.164	0.288	–0.14	–7.43E-07
Band 6	1.858	0.542	–0.38	Error
Band 7	2.259	0.561	–0.20	5%
(6611) 1993 VW	Centre (μm)	*FWHM* (μm)	Strength (natural log)	Continuum and error in fit
Band 1	0.392	0.276	–1.17	
Band 2	0.671	0.154	–0.25	Offset
Band 3	0.902	0.206	–0.70	0.47
Band 4	0.995	0.182	–0.25	Slope
Band 5	1.170	0.288	–0.21	–4.96E-07
Band 6	1.870	0.542	–0.51	Error
Band 7	2.250	0.560	–0.19	10%

considered to be a significant high-calcium pyroxene component. It is noticeable that asteroid (6611) 1993 VW presents a higher proportion of HCP relative to LCP than the other two objects. Note that the values of HCP/(HCP+LCP) for the eucrite Bouvante determined by Sunshine et al. (2004) agree with the electron microprobe modal analyses by Christophe Michel-Lévy et al. (1987), which obtained a value of 0.32. In the same paper, Sunshine et al. (2004) determined the HCP/(HCP+LCP) ratio for the V-type asteroid (4188) Kitezh to be 0.3–0.4, which is also consistent with the values for Bouvante. All these values are presented in Table 3 for comparison and are in agreement with the values of the three NEOs.

Finally, we must mention that plagioclase and high-calcium pyroxene both have absorptions bands near 1.2 μm. Given this ambiguity, it is difficult to infer the plagioclase content in the presence of HCP. Nonetheless, the absorption centered near 1.2 μm is relatively strong compared to the primary HCP absorption band at 1.0 μm (see Fig. 3), suggesting a relatively high proportion of plagioclase (Sunshine et al. 2004) in the composition of the three observed objects.

4. Conclusions

The mineralogical analysis performed on the spectra of three V-type NEOs give quite interesting and, sometimes, conflicting results. Initially, using a classical method developed by several authors and reviewed in G02, we derived a very similar low-calcium pyroxene composition (Wo_{7-9} Fs_{34-39}) for the three objects. We also obtained the indication that olivine can be present only in the surface of one of them, specifically (6611) 1993 VW. However, it is important to remember that these results must be taken with care due to several factors. First of all, the equations used to compute the [Wo] and [Fs] contents are valid only for a single pyroxene. Therefore, if our objects do have a surface dominated by a mixture of high- and low-calcium pyroxene mixture, then the derived [Wo] and [Fs] values can be unreal. Secondly, due to the calibrations, the obtained values present relatively large errors.

To have more insight into the mineralogy of the observed asteroids, we then applied the MGM method. Note that this method implies an a priori knowledge of the minerals present in the surface to be able to perform a fit between laboratory calibrations and the observed spectra. Due to this particularity of the method, equally plausible solutions can be obtained. In the case of the three NEOs, the best fit seem to indicate a mixture of low- and high-calcium pyroxene in a HCP/(HCP+LCP) ratio of around 30%. If this is true, then the [Wo] and [Fs] derived above are not real. However, the obtained result is highly dependent on the adopted chemistry of the fitted pyroxenes (SP93 in our case).

The performed analysis indicates that the surface of the three observed NEOs is composed either of a low-calcium pyroxene or of a mixture of low- and high-calcium pyroxene. Disregarding which one of these two determinations correctly represents the surface composition of the objects, it is important to note that each one derives a similar composition for the three asteroids. Moreover, both indicate that these objects plot in the Howardite region when considering their Band I vs. Band II centres (Fig. 2).

In the asteroid and meteorite communities, it is commonly accepted that the HED meteorites are most likely originally derived from (4) Vesta. Our results further strengthen the hypothesis of a genetic link between V-type NEOs and HED meteorites. However, we are still lacking a strong constraint on the origin of the basaltic achondrite NEOs. The results presented here indicate that these three NEOs could come either from (4) Vesta or from the same parent body as (1459) Magnya, as well as from another, still unknown, or already disappeared, body. We expect that the Dawn mission, obtaining a detailed mineralogical map of Vesta, will provide some answers to the problem of the origin of the V-type asteroids. On the other hand, more mineralogical

studies on the basaltic asteroids are certainly in need before we can derive secure conclusions.

Acknowledgements. We thank Mario Di Martino for providing the visible spectra of (6611) 1993 VW. We also thank M. Gaffey for his detailed review and comments that much improved the paper. Financial support by CNPq and FAPERJ during the present research is acknowledged.

References

Adams, J. B. 1974, JGR, 79, 4829
Adams, J. B. 1975, Interpretation of visible and near-infrared diffuse reflectance spectra of pyroxenes and other rock-forming minerals, ed. C. Jr. Karr, Infrared and Raman Spectroscopy of Lunar and Terrestrial Minerals, Academic, San Diego, 91
Baffa, C., Comoretto, G., Gennari, S., et al. 2001, A&A, 378, 722
Binzel, R. P., Lupishko, D., Di Martino, M., Whiteley, R. J., & Hahn, G. J. 2002, Physical Properties of Near-Earth Objects, ed. W. F. Jr. Bottke, A. Cellino, P. Paolicchi, & R. P. Binzel, Asteroid III (Tucson: Univ. of Arizona Press), 255
Burns, R. G. 1970, Am. Mineral., 55, 1608
Cloutis, E. A., & Gaffey, M. J. 1991, JGR, 96, E5, 22809
Cloutis, E. A., Gaffey, M. J., Jackowsky, T., & Reed, K. J. 1986, JGR, 91, B11, 11641
Colina, L., & Bohlin, R. 1997, AJ, 113, 1138
Christophe Michel-Lévy, M., Bourot-Denise, M., Palme, H., Spettel, B., & Wänke, H. 1987, Bull. Mineral., 199, 449
Cruikshank, D. P., Tholen, D. J., Bell, J. F., Hartmann, W. K., & Brown, R. H. 1991, Icarus, 89, 1
de León, J., Serra-Ricart, M., Licandro, J., & Dominguez, L. 2003, Monitoring and physical characterization of Near-Earth Objects, ed. Barbara Warmbein, Proc. ACM 2002, ESA-PD, 911
Di Martino, M., Manara, A., & Migliorini, F. 1995, A&A, 302, 609
Duffard, R., Lazzaro, D., Licandro, J., et al. 2004, Icarus, 171, 120
Duffard, R., Lazzaro, D., & de León, J. 2005, Meteoritics and Planetary Science, 40, 3, 445
Gaffey, M. J. 1997, Icarus, 127, 130
Gaffey, M. J., Bell, J. F., Brown, R. H., et al. 1993, Icarus, 106, 573
Gaffey, M. J., Cloutis, E. A., Kelley, M. S., & Reed, K. L. 2002, Mineralogy of Asteroids, ed. W. F. Jr. Bottke, A. Cellino, P. Paolicchi, & R. P. Binzel, Asteroid III (Tucson: Univ. of Arizona Press), 183
Hardersen, P. S., Gaffey, M. J., & Abell, P. A. 2004, Icarus, 167, 170
Kelley, M. S., Vilas, F., Gaffey, M. J., & Abell, P. A. 2003, Icarus, 165, 215
King, T. V. V., & Ridley, I. W. 1987, JGR, 92, 11457
Landolt, A. U. 1992, AJ, 104, 340
Licandro, J., Ghinassi, F., & Testi, L. 2002, A&A, 388, L9
Migliorini, F., Morbidelli, A., Zappala, V., et al. 1997, MAPS, 32, 903
Moroz, L., Schade, U., & Wasch, R. 2000, Icarus, 147, 79
Sunshine, J., & Pieters, C. 1993, JGR, 98, E5, 9075
Sunshine, J., Pieters, C., & Pratt, S. 1990, JGR, 95, B5, 6955
Sunshine, J., Bus, S. J., Burbine, T. H., McCoy, T. J., & Binzel, R. P. 2002, Unambiguous spectral evidence for high- (and low) calcium pyroxene in asteroids and meteorites, in LPS XXX, Abs. #1356 (Houston: Lunar and Planetary Institute)
Sunshine, J., Bus, S. J., McCoy, T. J., et al. 2004, MAPS, 39, 1343
Vernazza, P., Mothé-Diniz, T., Barucci, M. A., et al. 2005, A&A, 436, 1113